Development of a frequency-stabilized 555.8-nm laser

Min Zhou (周 敏), Liangyu Huang (黄良玉), and Xinye Xu (徐信业)*

State Key Laboratory of Precision Spectroscopy and Department of Physics, East China Normal University, Shanghai 200062, China

**Corresponding author: xyxu@phy.ecnu.edu.cn*

Received July 16, 2013; accepted October 17, 2013; posted online December 5, 2013

Experiments on developing a frequency-stabilized 555.8-nm laser are presented. The 555.8-nm laser is obtained by frequency doubling of a 1111.6-nm diode laser through single-passing a periodically poled lithium niobate (PPLN) waveguide. The 555.8-nm laser is then locked to a stable high-finesse Fabry–Perot (FP) cavity by the Pound–Drever–Hall (PDH) technique. The finesse of the cavity is measured by the heterodyne cavity ring-down spectroscopy technique. The linewidth of the 555.8-nm laser is investigated. After the laser is locked, the laser line width is reduced to about 3 kHz. This frequency-stabilized 555.8-nm laser is used in experiments on the laser cooling and trapping of ytterbium atoms to develop an ytterbium optical clock.

OCIS codes: 140.3425, 140.3515, 300.6210, 020.3320.
doi: 10.3788/COL201311.121402.

Frequency-stabilized light sources are essential in a wide range of applications, such as atomic clocks, gravitational-wave detection, and quantum information processing[1−3]. Significant efforts have recently been made to improve the performance of optical atomic clocks and achieve the recommended accuracy of 10^{-18}[4−7]. In an ytterbium optical atomic clock, second-stage cooling relying on the 555.8-nm $^1S_0$–$^3P_1$transition must be performed after the broadband 399-nm $^1S_0$–$^1P_1$ cooling process so that the atoms can be cooled down to the microkelvin level, which is adequately cold for loading atoms efficiently into the optical lattices. Given that this intercombination transition has a natural linewidth of 182 kHz, a frequency-stabilized laser with a much narrower linewidth is required for second-stage cooling. To the best of our knowledge, stable 555.8-nm light sources have been developed by locking to an external cavity[8,9], an ytterbium atomic transition[10,11], or a phase-locked fiber comb[12].

In this letter, we report experiments on developing a frequency-stabilized 555.8-nm laser system forming part of a ^{171}Yb optical lattice clock. The 555.8-nm laser is frequency stabilized to a high-finesse Fabry–Perot (FP) cavity by the Pound–Drever–Hall (PDH) technique to reduce the laser linewidth to about 3 kHz. The proposed frequency-stabilized 555.8-nm laser system is successfully used in the laser cooling and trapping of ytterbium atoms in an ^{171}Yb optical clock and may be applied for building ^{174}Yb optical clocks.

The 555.8-nm light is generated by the second harmonic generation (SHG) of a 1111.6-nm laser, as shown in Fig. 1. A periodically poled lithium niobate (PPLN) waveguide is used for frequency doubling. A 1111.6-nm diode laser (DL Pro, Toptica Photonics AG, Germany) with a linewidth of 1 MHz is injected into a fiber amplifier (Keopsys Inc, French) through a fiber. The power-amplified 1111.6-nm laser is then inputted directly into the waveguide through the fiber connection. The PPLN crystal is held in a temperature controlled oven (LDT-5525B, ILX Lightwave Corp, USA) with an uncertainty of 0.1 °C.

A high-finesse FP cavity (ATFilms Inc, USA) is used to stabilize the frequency of the 555.8-nm laser. The linear cavity consists of two high-reflectivity mirrors optically connected by a 10-cm-long spacer entirely made of ultra-low expansion material. It is a half-symmetric resonator constructed from a plane mirror and a 50-cm radius concave mirror. The free spectral range (FSR) of the cavity is 1.5 GHz. The cavity is placed horizontally inside a vacuum chamber ($\sim 10^{-5}$ Torr) pumped by an ion pump, and the cavity temperature is stabilized at 22.005 °C with an uncertainty of 0.002 °C.

The PDH locking technique[13,14] is utilized to stabilize the frequency of the 555.8-nm laser. A schematic of the experimental setup is shown in Fig. 1. Using a $\lambda/2$ waveplate and a polarizing beam splitter (PBS1), part of the 555.8-nm laser is sent to the frequency-locking system. The laser firstly goes through a double-pass

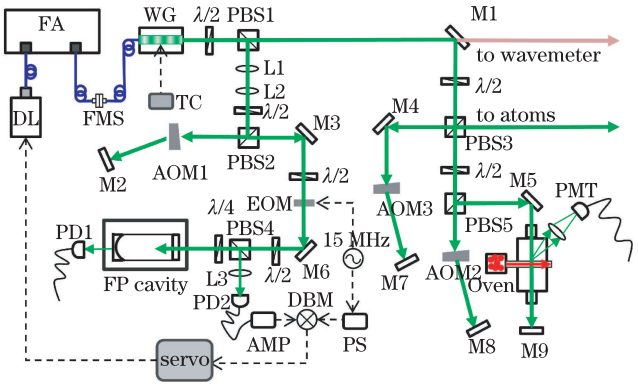

Fig. 1. (Color online) Schematic of the experimental setup. A waveguide (WG) is used for second harmonic generation. The high-finesse Fabry Perot (FP) cavity is used to lock the laser frequency. DL: diode laser; FA: fiber amplifier; FMS: fiber mating sleeve; TC: temperature controller; $\lambda/2(\lambda/4)$: half (quarter) waveplate; PBS: polarizing beam splitter; L (M): lens (mirror); AOM (EOM): acousto-optic (electro-optic) modulator; AMP: radio frequency amplifier; DBM: double-balanced mixer; PS: phase shifter; PD: photodetector; PMT: photomultiplier tube.

 © 2013 Chinese Optics Letters

acoustic-optic modulator (AOM1) with a radio frequency (RF) of 80 MHz and then passes a home-made electro-optic modulator (EOM) with a modulation frequency of 15 MHz and a modulation index of $\beta \approx 0.65$. The double-pass AOM configuration maintains the output-beam propagating direction during laser frequency tuning. Sidebands at 15 MHz are added to the incident laser by introducing phase modulation. Residual amplitude modulation induced by the birefringence effect of the electro-optic crystal may cause baseline drifts of the PDH error signal. To reduce this effect, a $\lambda/2$ waveplate is added to the front of the EOM to allow selection of the optimal light-polarization direction.

Mode matching is critical for transferring a maximum power into the fundamental TEM_{00} mode in the reference cavity. Two convex lenses (L1 and L2) are added to adjust the input beam size and divergence to match the cavity mode. The focal lengths of two lenses are f_1= 50 mm and f_2=40 mm. The beam waist of the laser after the two lenses is measured by a beam quality analyzer. The positions of the two mode-matching lenses are determined by a simple ABCD (i.e., ray transfer) matrix. Over 80% of the laser power can be transferred to the fundamental TEM_{00} mode in the cavity.

In our experiment, the power of the 555.8-nm laser in the cavity is about 27.5 μW. A photodetector (PD1) is placed behind the cavity to monitor transmission signals. The reflection beam from the front mirror of the cavity is extracted by a $\lambda/4$ waveplate and PBS4, which is finally focused on a fast low-noise photodetector (PD2) with a bandwidth of 1.2 GHz by a lens. The direct current (DC) component of the reflection signal can be monitored by simply replacing PD2 with a DC-coupled photodetector, and the 15-MHz signal from PD2 is amplified by a low noise RF amplifier. This amplified signal is demodulated to produce an error signal with a double-balanced mixer (DBM) against the RF signal that drives the EOM as well. Finally, the dispersion-shaped error signal is split into two parts: one is filtered by a proportional-integral-differential controller to feed on the piezoelectric transducer (PZT) of the 1111.6-nm diode laser as slow feedback while the other is directly sent to the electric-current controller of the 1111.6-nm diode laser as fast feedback.

Given that the 555.8-nm laser light cools and traps the ^{171}Yb atoms, its frequency must be close to the resonant frequency of the $^1S_0-{}^3P_1$transition. Therefore, the cavity mode closest to the resonant frequency must firstly be determined, after which the 555.8-nm laser frequency is locked to this cavity mode. Another 555.8-nm laser beam is allowed to interact with a thermal Yb atomic beam, as shown in Fig. 1. The laser beam firstly goes through the double-pass AOM2 with a RF frequency of 80 MHz, similar to that in AOM1, and then travels into a vacuum chamber intersecting the ytterbium atomic beam at an angle of 90°. The power of the input laser is about 0.3 mW, and the ytterbium atomic beam effuses from an oven heated at a temperature of 380 °C. A photomultiplier tube (PMT) is perpendicularly mounted above this interaction area to observe fluorescence signals.

In the experiment, a wavemeter is firstly used to measure the frequency of the 555.8-nm laser, after which the frequency of the 555.8-nm laser is allowed to approach the resonant transition frequency as closely as possible by manually adjusting the PZT voltage of the 1111.6-nm diode laser. The fluorescence signal corresponding to the transition $^1S_0(F=1/2)$-$^3P_1$ (F'=3/2) can be obtained by electronically scanning the PZT voltage of the 1111.6-nm diode laser and looking for the fluorescence signals with the PMT. Furthermore, one cavity mode is allowed close to the fluorescence-signal peak of the transition $^1S_0(F=1/2)$-$^3P_1$ (F'=3/2) by adjusting the RF frequencies of AOM1 and AOM2. Finally, the 555.8-nm laser frequency is locked to this typical cavity mode. The third part of the 555.8-nm laser is also firstly sent through the double-pass AOM3 with a RF frequency of 80 MHz and then delivered to the 555.8-nm magneto-optic trap (MOT) for cooling and trapping ytterbium atoms; its frequency detuning is controlled by the AOM3, as shown in Fig. 1. The linear frequency drift of the FP cavity can be cancelled by tuning the AOM1 frequency before every locking process. In experiments with intervals of one week, the cavity drift is at most 200 kHz. For daily experiments, manual correction is unnecessary.

Figure 2 shows the dependence of the SHG output power on the fundamental power. The conversion efficiency decreases when the fundamental power is over 120 mW. As mentioned in our previous theoretical work[15], high fundamental light intensities result in thermally induced dephasing effects and nonlinear absorption, which may be main factors influencing conversion efficiency degradation of a waveguide. Given that the SHG output power is sensitive to the crystal temperature because of the phase matching condition, the SHG power is measured as a function of the temperature of the crystal, as shown in the inset of Fig. 2, where the fundamental power is set to about 190 mW.

The plot of the 555.8-nm laser output power as a function of crystal temperature shows typical sinc^2-function behavior. The measured full width at half maximum of the center peak is about 1.3 °C, and the optimal temperature where the 555.8-nm laser output power is maximized is 36.8 °C. A temperature stability of 0.1 °C around the optimal temperature controls the fluctuations of the SHG output power to less than 0.3%. Given that the input power of the 1111.6-nm laser cannot exceed the

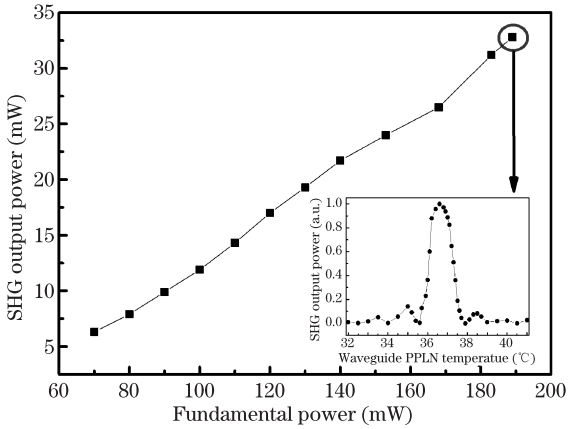

Fig. 2. (Color online) SHG output power as a function of the fundamental power. The inset shows the SHG output powers at different phase-matching temperatures ranging from 32 °C to 41 °C.

safety value of 200 mW, which is required by the manufacturer, a laser power of about 30 mW at 555.8-nm can be obtained.

The finesse of the FP cavity is measured by the heterodyne cavity ring-down spectroscopy technique[16], as shown in Fig. 3. The RF power is not applied on the EOM during this measurement. By rapidly sweeping the PZT of the 1111.6-nm diode laser, the reflection signal detected by PD2 will oscillate with an exponentially decaying envelope. The ring-down time extracted by fitting of the data is about 3 μs, and the finesse of the cavity is estimated to be about 15000.

Figure 4 shows the transmission signals and the PDH error signals before and after the 555.8-nm laser is locked. The inset in Fig. 4 shows the DC component of the reflection signal from the cavity. The reflection signal shows a dip that is never close to zero, which is attributed to the fact that the transmission through the input mirror is not equal to the total loss within the cavity, thereby resulting in low coupling efficiency. Nevertheless, it is less important than minimizing the loss to achieve high finesse in the cavity and obtain high signal-to-noise ratio (SNR) error signals for robust laser frequency stabilization.

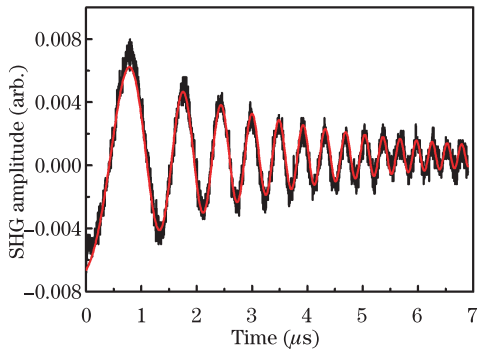

Fig. 3. (Color online) Recorded swept-laser cavity ring-down signals from the optical heterodyne beat of the decaying cavity field and the reflection laser field. By fitting the measured data, we find that the ring-down time is about 3 μs.

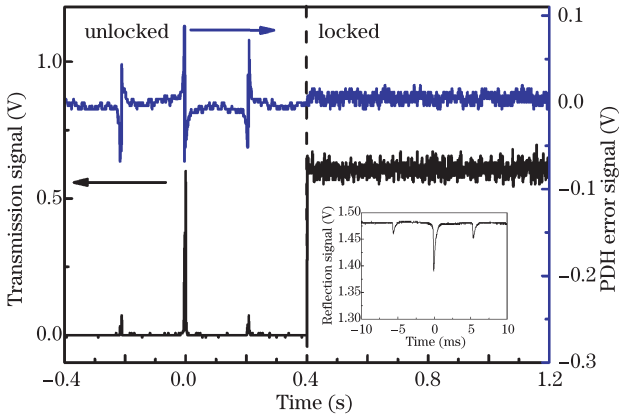

Fig. 4. (Color online) Transmission and PDH error signals in two cases. In the first case, the two signals present a carrier-sideband shape and a dispersive shape when the laser is unlocked, as shown in the left. In the inset, the reflection signal shows three carrier-sideband dips. In the second case, the transmission signal is flat and remains at the peak of the signal when the laser is locked, as shown in the right.

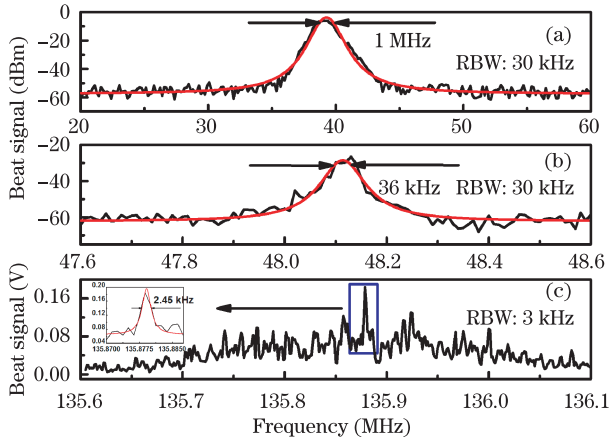

Fig. 5. (Color online) Spectra of beatnotes between the 555.8-nm laser and another laser. (a) Both 555.8-nm lasers are free-running. The fitted −3-dB linewidth is 1 MHz, as measured at a RBW of 30 kHz. (b) The 555.8-nm laser is locked but the second 555.8-nm laser remains free-running. The beatnote linewidth is about 36 kHz, as measured at an RBW of 30 kHz. (c) The locked 555.8-nm laser beats with a phase-locked titanium-sapphire-type frequency comb. The inset shows that the 555.8-nm laser has a linewidth of about 3 kHz as measured at an RBW of 3 kHz after frequency stabilization. RBW: resolution of bandwidth.

To demonstrate that the laser is well locked to the $^1S_0-^3P_1$ transition of the desired ytterbium isotope, fluorescence signals from the PMT are monitored. By finely tuning the frequency of AOM1, the locking point of the PDH error signal is aligned to the peak of the fluorescence signal. When the laser is locked, the PMT signal (not depicted in Fig. 4) stays at the peak of the fluorescence signal. PD1 signal is flat and remains at the peak, as shown in Fig. 4, which indicates that the 555.8-nm laser is resonant with the atomic transition. After the laser is frequency stabilized, the frequency jitter is reduced. By adjusting the frequency of AOM3 relative to that of AOM2, correct frequency detuning of the 555.8-nm laser for laser cooling experiments can be achieved.

Using another similar 555.8-nm laser system, the 555.8-nm laser linewidth can be measured. The second 555.8-nm laser is used in our second series of ytterbium atomic clock experiments and kept perpetually free-running during the measurements; the linewidth of this laser is about 50 kHz. The beatnotes between the two 555.8-nm lasers with and without locking of the original 555.8-nm laser are shown in Figs. 5(a) and (b), respectively. In Fig. 5(a), both lasers are free-running. The beatnote signal shows a –3-dB linewidth of about 1 MHz at a resolution bandwidth (RBW) of 30 kHz by Lorentzian fitting. In Fig. 5(b), the 555.8-nm laser is locked to the FP cavity, whereas the second 556.8-nm laser remains free-running. In this system, the –3-dB linewidth is about 36 kHz at a RBW of 30 kHz and Lorentzian fitting. This finding implies that the linewidth of the original 555.8-nm laser is less than 50 kHz, and its frequency jitter is mostly suppressed after frequency stabilization.

The beatnote between the locked 555.8-nm laser and a titanium-sapphire-type frequency comb is measured, as shown in Fig. 5(c). The optical comb is phase-locked to a 1064-nm laser referenced to an ultra-stable FP cavity.

The linewidth of the l064-nm laser is about 1 Hz, which is transferred to the optical comb. Each frequency component around 555.8-nm has a linewidth of about 1 Hz, which is much narrower than the linewidth of the locked 555.8-nm laser. Figure 5(c) shows that the observed linewidth of the beat signal is about 3 kHz at a RBW of 3 kHz by Lorentzian fitting; thus, the linewidth of the frequency stabilized 555.8-nm laser is about 3 kHz. Given that the natural linewidth of the $^1S_0-^3P_1$ transition of ytterbium atoms is 182 kHz, this laser has adequate properties to achieve second-stage cooling in the Yb atomic clock experiment. The 555.8-nm laser shows frequency instability in the 10^{-12} level at an average time of 1 s.

In our experiment, the 555.8-nm laser can be locked to the FP cavity for one day. This frequency stabilized 555.8-nm laser may be used to cool and trap ytterbium atoms successfully in the second MOT. Thus, large numbers of cold atoms may be loaded in the optical lattices. The $^1S_0-^3P_0$ clock-transition spectrum of ^{171}Yb atoms has recently been observed to feature good SNRS, which is very helpful for developing an ytterbium optical clock in our laboratory.

In conclusion, we develope a frequency-stabilized 555.8-nm laser to achieve the second-stage cooling of ytterbium atoms. Using a SHG with the PPLN waveguide, a 555.8-nm laser with an output power of about 30 mW is generated. This laser frequency is then locked to a high-finesse FP cavity, and a linewidth of about 3 kHz is obtained. The proposed system shows excellent results in our ytterbium optical clock experiments.

The authors would like to thank Su Fang for her help. This work was supported by the National "973" Program of China (Nos. 2012CB821302 and 2010CB922903), the National Natural Science Foundation of China (Nos. 11134003 and 10774044), and Shanghai Excellent Academic Leaders Program of China (No. 12XD1402400).

References

1. T. Kessler, C. Hagemann, C. Grebing, T. Legero, U. Sterr, F. Riehle, M. J. Martin, L. Chen, and J. Ye, Nat. Photon. **6,** 687 (2012).
2. A. Abramovici, W. E. Althouse, R. W. Drever, Y. Gürsel, S. Kawamura, F. J. Raab, D. Shoemaker, L. Sievers, R. E. Spero, K. S. Thorne, R. E. Vogt, R. Weiss, S. E. Whitcomb, and M. E. Zucker, Science **256,** 325 (1992).
3. C. Monroe, Nature **416,** 238 (2002).
4. J. A. Sherman, N. D. Lemke, N. Hinkley, M. Pizzocaro, R. W. Fox, A. D. Ludlow, and C. W. Oates, Phys. Rev. Lett. **108,** 153002 (2012).
5. M. Yasuda, H. Inaba, T. Kohno, T. Tanabe, Y. Nakajima, K. Hosaka, D. Akamatsu, A. Onae, T. Suzuyama, M. Amemiya, and F. L. Hong, Appl. Phys. Express **5,** 102401 (2012).
6. M. D. Swallows, M. J. Martin, M. Bishof, C. Benko, Y. G. Lin, S. Blatt, A. M. Rey, and J. Ye, IEEE Trans. Ultrason. Ferroelectr. Freq. Control **59,** 416 (2012).
7. R. L. Targat, L. Lorini, Y. L. Coq, M. Zawada, J. Guéna, M. Abgrall, M. Gurov, P. Rosenbusch, D. Rovera, B. Nagórny, R. Gartman, P. G. Westergaard, M. E. Tobar, M. Lours, G. Stantarelli, A. Clairon, S. Bize, P. Laurent, P. Lemonde, and J. Lodewyck, Nat. Commun. **4,** 2109 (2013).
8. S. Uetake, A. Yamaguchi, S. Kato, and Y. Takahashi, Appl. Phys. B **92,** 33 (2008).
9. C. Y. Park, D. H. Yu, W. K. Lee, S. E. Park, and E. B. Kim, in *Proceedings of Conference on Precision Electromagnetic Measurements Digest* 186 (2008).
10. C. Abou-Jaoudeh, C. Bruni, F. Baumer, and A. Gorlitz, in *Proceedings of 2009 IEEE International Frequency Control Symposium Jointly with the 22nd European Frequency and Time Forum* 756 (2009).
11. K. Pandey, K. D. Rathod, S. B. Pal, and V. Natarajan, Phys. Rev. A **81,** 033424 (2010).
12. M. Yasuda, T. Kohno, H. Inaba, Y. Nakajima, K. Hosaka, A. Onae, and F. L. Hong, J. Opt. Soc. Am. B **27,** 1388 (2010).
13. E. D. Black, Am. J. Phys. **69,** 79 (2001).
14. R. Drever, J. L. Hall, F. V. Kowalski, J. Hough, G. M. Ford, A. J. Munley, and H. Ward, Appl. Phys. B **31,** 97 (1983).
15. G. H. Li and X. Y. Xu, Chin. Opt. Lett. **9,** 121901 (2011).
16. Y. B. He and B. J. Orr, Chem. Phys. Lett. **335,** 215 (2001).